International Symposium COMODIA 90: 437-442(1990)

The Effects of "Inclination Angle of Swirl Axis" on Turbulence Characteristics in a 4-Valve Lean-Burn Engine with SCV

S.Furuno, S.Iguchi, K.Oishi and T.Inoue

Toyota Motor Corporation
1200 Mishuku
Susono 410-11
Japan

ABSTRACT

It has been demonstrated that the in-cylinder turbulence of a 4 valve engine with a swirl control valve (SCV) is enhanced by inclined swirl. This paper examines the effects on turbulence of varying swirl inclination angle defined as the inverse tangent of the vertical component of total angular momentum divided by the horizontal component. Experiments were conducted on a 4-valve single cylinder engine with SCV using a backward-scatter LDV and BSA (Burst Spectrum Analyzer). The results show that although total angular momentum is greatest with horizontal swirl, turbulence intensity measured in the center of the combustion chamber attains a peak value when the swirl inclination angle is between 30 and 45 degrees from the cylinder axis under the same air flow rate.

INTRODUCTION

In the case of a gasoline fueled vehicle, lean burn drastically reduces fuel consumption but NOx emissions are higher than those with stoichiometric air fuel ratio and a 3-way catalyst. It would therefore seem that the approach that is most capable of satisfying both demands is to develop a lean burn engine that will operate in the leaner air fuel ratio domain of lower NOx level. Toyota has pioneered the development of the lean burn engine and in 1990 introduced a 1.6L, 4-valve lean-burn engine into the market(1).

When developing the original 4-valve lean-burn engine, we designed the intake port with SCV to increase turbulence generation by inclining the swirl axis (inclined swirl)(2). This paper describes studies subsequently conducted to enhance our understanding of the effects of inclined swirl on turbulence characteristics by introducing "the inclination angle of swirl axis" as an index to optimize the gas swirl.

TEST ENGINE & INTAKE PORTS

Test Engine

Motoring tests were conducted on a 4-valve single cylinder engine. The combustion chamber was of the pent roof type and the piston surface was flat. The diameters of the intake and exhaust valves were 30mm and 26mm respectively. For LDV measurement purposes, the spark plug hole located very close to the bore center was replaced by a quartz window (diameter 14mm).

Table 1 Engine Specifications

Engine type	four-stroke
Bore x Stroke	81mm x 78mm
Compression ratio	7.8
Valve lift	6.6mm
Intake valve timing	BTDC 6° ~ ABDC 59°
Exhaust valve timing	BBDC 50° ~ ATDC 6°

Intake Port Configurations

Fig.1 shows the two intake port configurations. In both configurations one of the ports was a straight port closed by a swirl control valve (SCV). To generate swirl as close as possible to horizontal, a helical port was adopted for configuration I (Fig.1a). And in order to easily vary swirl inclination angle, a straight port fitted with a shroud was used in configuration II (Fig.1b). Swirl inclination angle was varied by changing the shroud direction, which is defined as the angle α between the horizontal line bisecting the shroud and the line passing through the centers of the valve and the bore(11).

To prevent rotation of the shrouded valve, a

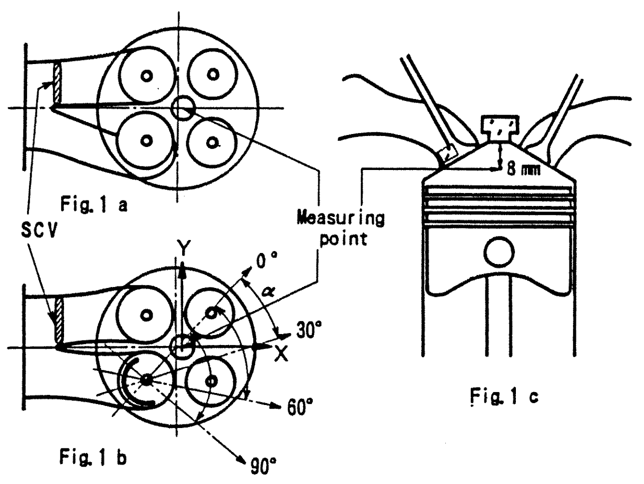

Fig.1 Intake port configurations

small pin was provided on the valve stem, and channels into which the pin could be slotted were provided in the valve guide.

Four shroud directions α were tested: 0°, 30°, 60° and 90°. Hence five swirl inclination angles in all were studied (Fig.1a, Fig.1b). The helical port of configuration I was designed so as to produce the same differential pressure as the straight port of configuration II.

Fig.1c shows the measuring point in the combustion chamber. The point was decided to investigate the turbulence characteristics at almost the central position of the combustion volume at TDC.

MEASUREMENT OF SWIRL INCLINATION ANGLE

Measurement Method

Since it is impossible to measure the actual swirl inclination angle, a suitable measurement method had to be devised. Visualization was considered but it was found that the angle could not be precisely determined. It was therefore decided to measure the vertical and horizontal components of angular momentum and to calculate the inclination angle. Accordingly, for each of the five generated swirls, steady flow tests were conducted and the vertical and horizontal components were measured using an impulse swirl meter. Fig.2 shows the test rigs for simulating air flow at BDC in an actual engine. In both cases, the vertical distance ℓ from the undersurface of the cylinder head to the center of the impulse swirl meter was about 1.5 times cylinder bore diameter, and air flow rate through the intake port was 20g/sec.

When setting up the test apparatus shown in Fig.2b, measurements were taken while rotating the cylinder head through one full turn on the cylinder so as to determine the position yielding the maximum value for the vertical component.

The data recorded in these flow tests were averaged to obtain values for calculating the swirl inclination angles. The mean values for the vertical component were doubled because the air flow rate through the impulse swirl meter was controled by the flow control valve as half of the total flow rate through the intake port.

Calculation

The swirl inclination angle θ was calculated using the following equation:

$$\theta = \mathrm{Tan}^{-1} \ (\Omega v / \Omega h) \qquad (1)$$

where Ωv and Ωh are respectively the vertical and horizontal components of the total angular momentum Ω.

The total angular momentum of the bulk gas motion was calculated as follows:

$$\Omega = \sqrt{\Omega v^2 + \Omega h^2} \qquad (2)$$

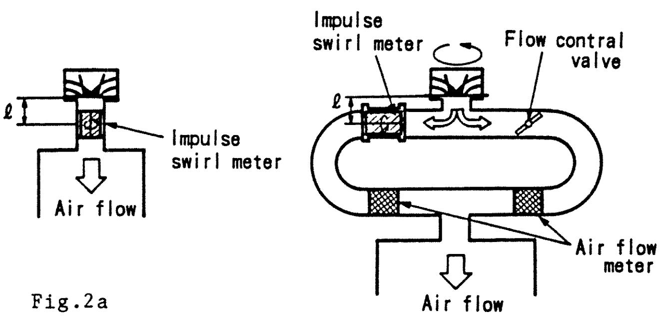

Fig.2a Horizontal component

Fig.2b Vertical Component

Fig.2 Test rings for measurement of angular momentum

MEASUREMENT OF TURBULENCE

The characteristics of the turbulence in each

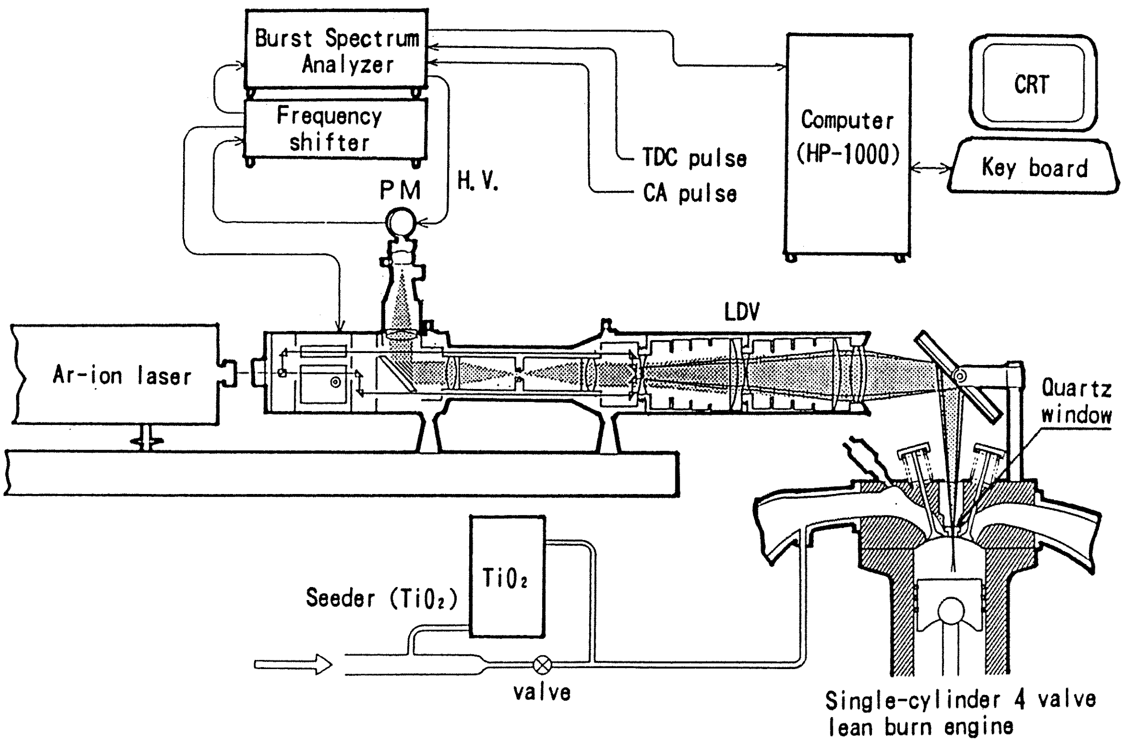

Fig.3 Backward-scatter LDV system

cycle were ascertained from instantaneous velocities measured along the X and Y axes in the horizontal plane by LDV[(3)~(7)].

Experimental Apparatus & Procedure

A dual-beam, backward-scatter LDV optical system with Ar-ion laser source was mounted on a stand providing manual traverses in the X, Y and Z axes. The dual laser beams were introduced into the combustion chamber via an adjustable mirror located above the cylinder head as shown in Fig.3. For precise determination of turbulence characteristics within a single cycle, a high signal to noise ratio is essential. Features of this LDV optical system which significantly improve S/N are the double beam expanders and the small pinhole located in front of the photomultiplier. The signal processor was a Burst Spectrum Analyzer. Under motoring condition, the maximum valid data rate was 20kHz, the data validity rate being 70% with backward-scatter mode.

Table 2 LDV System Specifications

Ar-ion laser (Spectra-physics)	
wave length	514.5nm
power	1.2W
LDV optics (DANTEC)	
Focal length	600mm
Beam intersection angle	7.3°
Fringe spacing	4.02μm
Measuring volume diameter (as viewed through pinhole)	50μm
Signal processor (DANTEC)	
Burst Spectrum Analyzer	
Frequency shift	40MHz
Seeding rig	
Principle: Brushing single particles off a dense bulk of powder.	
Particles: TiO_2 (Mean diameter 0.3μm)	

All measurements were taken under a motoring condition of 1200 rev/min. In order to keep the quartz window clear, no lubricating oil was supplied to the piston or cylinder head when measurements were taken. The measuring point was 8mm below the undersurface of the quartz window and 3mm from the bore center (see Fig.1c). Although fixed in terms of cylinder geometry, the relative position of the measuring point changed in relation to the bulk gas motion as the piston rose and fell.

Data Processing

The instantaneous velocity binary signals from the BSA were processed by a mini-computer (HP 1000/A-600). Turbulence characteristics were ascertained as outlined in Fig.4. For each cycle, valid data rate for the period 30°BTDC ~ TDC was equal to or greater than 7.2kHz. The bulk flow velocity U was calculated from the instantaneous velocities Ui by means of the moving average method[(8)]. The bulk flow was subtracted from the instantaneous velocities to obtain their high frequency components. From these high frequency components, turbulence intensity u was calculated using the moving root mean square method. For purposes of comparison, three cut-off frequencies were employed: 150Hz, 300Hz and 450Hz. In addition a power spectrum Pk was obtained by Fast Fourier Transformation of the instantaneous velocities. Mean bulk flow velocity $\overline{U}$, mean turbulence intensity $\overline{u}$, turbulence intensity cycle to cycle variation $\overline{\overline{u}}$ and the mean power spectrum $\overline{Pk}$ were obtained by ensemble averaging of the data for 100 cycles. The relevant equations are as follows:

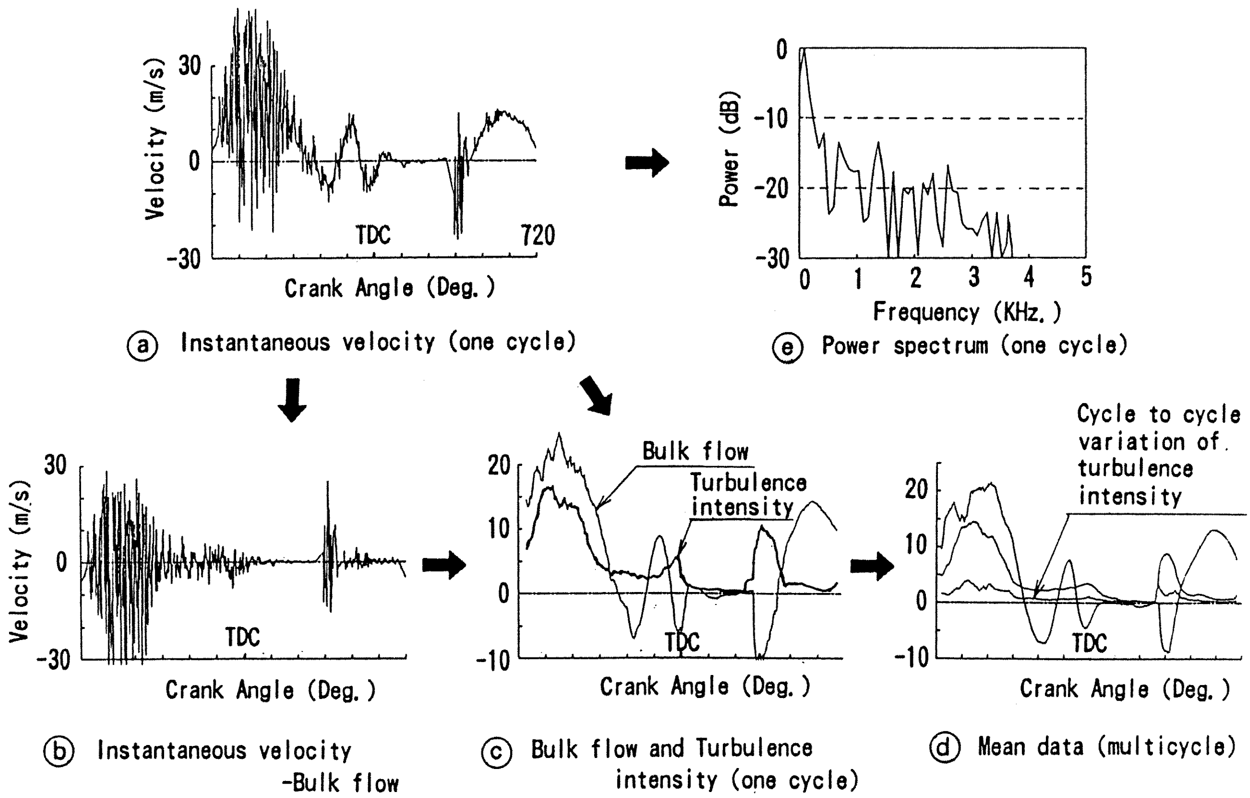

Fig.4 Determination of turbulence characteristics

$$U(n,\theta j,\Delta\theta)=\frac{1}{\Delta Zj}\sum_{k=1}^{\Delta Zj} Ui(n,\theta j,\Delta\theta,k) \tag{3}$$

$$u(n,\theta j,\Delta\theta)=\left[\frac{1}{\Delta Zj}\sum_{k=1}^{\Delta Zj}\{Ui(n,\theta j,\Delta\theta,k)-U(n,\theta j(k),\Delta\theta)\}^2\right]^{1/2} \tag{4}$$

$$\overline{U}(\theta j,\Delta\theta)=\frac{1}{N}\sum_{n=1}^{N} U(n,\theta j,\Delta\theta) \tag{5}$$

$$\overline{u}(\theta j,\Delta\theta)=\frac{1}{N}\sum_{n=1}^{N} u(n,\theta j,\ \Delta\theta) \tag{6}$$

$$\overline{\overline{u}}(\theta j,\Delta\theta)=\left[\frac{1}{N}\sum_{n=1}^{N}\{u(n,\theta j,\Delta\theta)-u(n,\theta j,\Delta\theta)\}^2\right]^{1/2} \tag{7}$$

$$Pk(n)=10\log\left[\{Re[Ck(n)]\}^2+\{Im[Ck(n)]\}^2\right] \tag{8}$$

$$Ck(n)=\frac{1}{Z_0}\sum_{t=0}^{Z_0-1} Ui(n,t)\exp\left(-\frac{i2\pi}{Z_0}kt\right)\qquad k=0,1,2,\cdots Z_0-1 \tag{9}$$

$$\overline{Pk}=\frac{1}{N}\sum_{n=1}^{N} Pk(n) \tag{10}$$

where n is the factor representing a cycle, N is the number of cycles, $\Delta\theta$ is the moving window of the crank angle, θj is the center of $\Delta\theta$, ΔZj is the number of the instantaneous velocity data in $\Delta\theta$, $\theta j(k)$ is the crank angle timing at which the instantaneous velocity is measured, Ck is the coefficient of FFT, Zo is half of the sampling number.

EXPERIMENT RESULTS

Swirl Inclination Angle

Fig.5 shows the results of the air flow tests. As can be seen, the swirl inclination angle θ varies from 90° when the shroud direction α is 0°, to 31° when the shroud direction is α 90°. With the helical port, swirl inclination angle θ is 19°. The computed magnitudes of angular momentum and of the vertical and horizontal components are plotted against swirl inclnation angle in Fig.6. The total angular momentum is not constant even though the flow rate was the same in all cases. This is because the magnitude of the vertical component does not increase linearly as swirl inclination angle changes (as is the case with the horizontal component) but has a peak between the swirl inclination angle of 40° and 60°. It is thought that the shape of the cylinder is not conducive to vertical swirl, i.e. whereas the cylinder is round in the horizontal plane, it is square in the vertical plane.

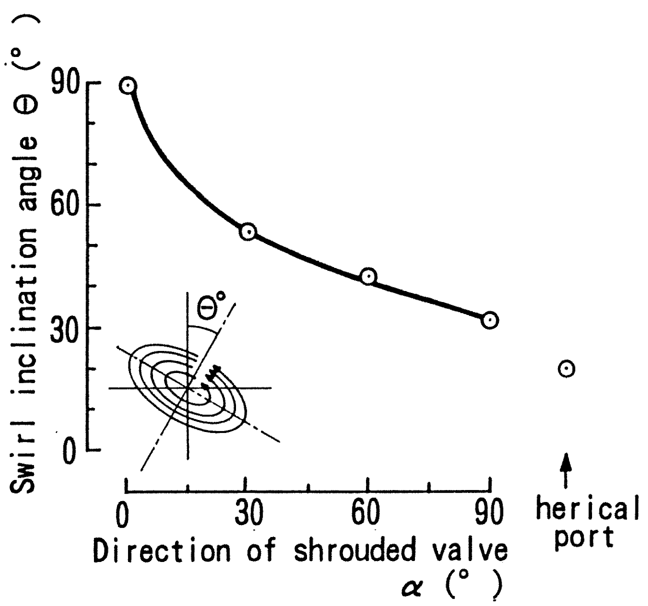

Fig.5 Air flow test results I: Swirl inclination angle

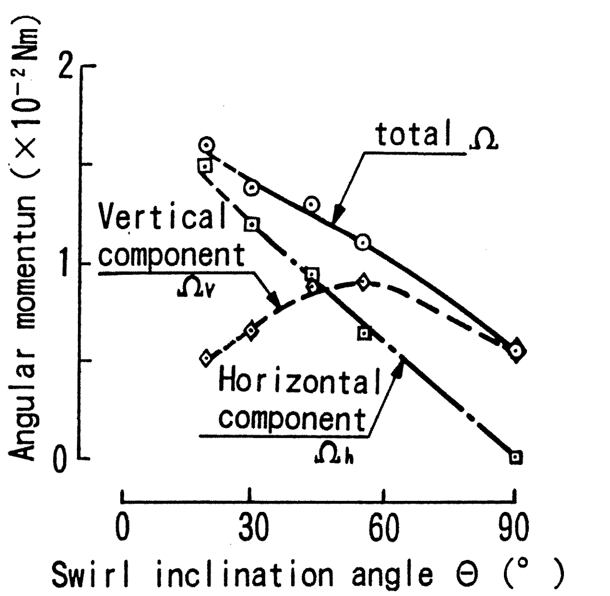

Fig.6 Air flow test results II: Angular momentum

Effect of Swirl Inclination Angle on Turbulence Intensity

Fig.7 shows the effects of swirl inclination angle on mean turbulence intensity (cut-off frequency 300Hz). During the period of initial combustion, 30°BTDC ~ TDC of the compression stroke (Fig.7a ~ 7c), turbulence intensity varies greatly according to swirl inclination angle, the peak value being attained when θ is between 30° and 45°(9). During the later stage of combustion, TDC ~ ATDC30°(Fig.7d ~ 7f), turbulence intensity is lower but the overall trend is very much the same: a peak value occurs between swirl inclination angles 30° and 45°.

It will be noted from Fig.7c and 7f that the cycle to cycle variation also peaks at the inclination angle corresponding to maximum turbulence. However the variation rate indicated by the normalized curves is lowest at this angle. Firing tests will therefore be necessary to ascertain to what extent combustion will be affected by the cyclical variation.

The assessment of turbulence intensity tends to vary according to the cut-off frequency. In Fig.8 the mean turbulence intensity (X axis component) is plotted against swirl inclination angle for cut-off frequencies of 150, 300 and 450Hz. The curves for 300Hz and 450Hz have the same shape and peak at the same angle. Moreover the cycle to cycle variation curves for these two frequencies coincide.

Fig.9 shows the mean power spectra up to 3.6kHz for the period from BTDC 90° (compression stroke) ~ ATDC38°. Throughout the entire frequency range, values for swirl inclination angles 31° and 43° are high and those for 19°, 54° and 90° are low. These results are in agreement with Fig.7.

BTDC

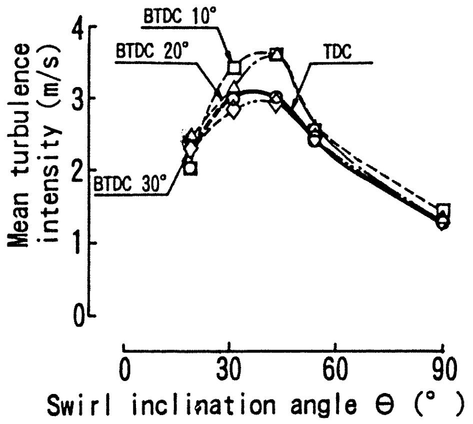

Fig. 7a X component

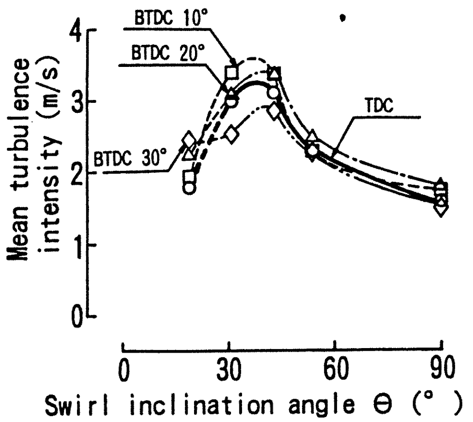

Fig. 7b Y component

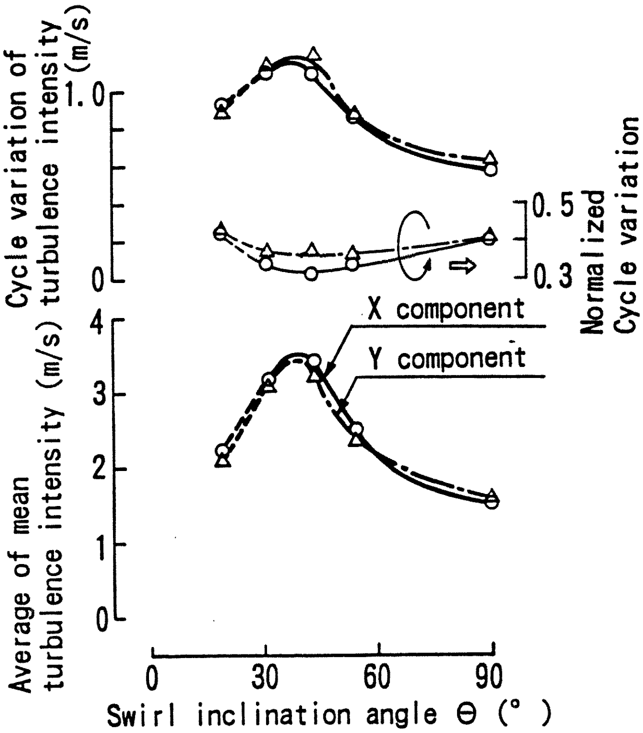

Fig. 7c Comparison of X & Y components

(Average of mean value for each degree of crank angle from 30°BTDC to TDC)

ATDC

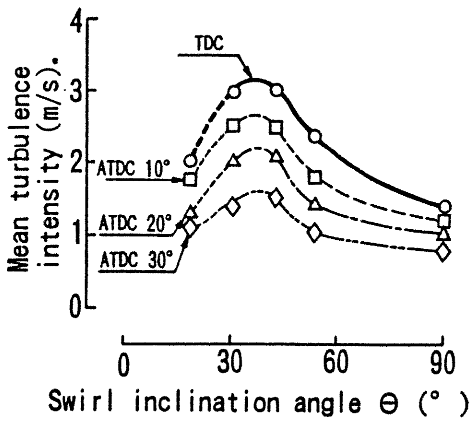

Fig. 7d X component

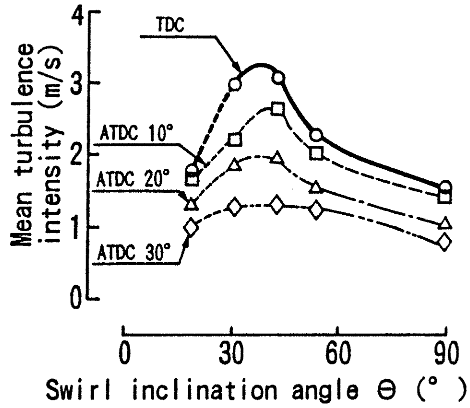

Fig. 7e Y component

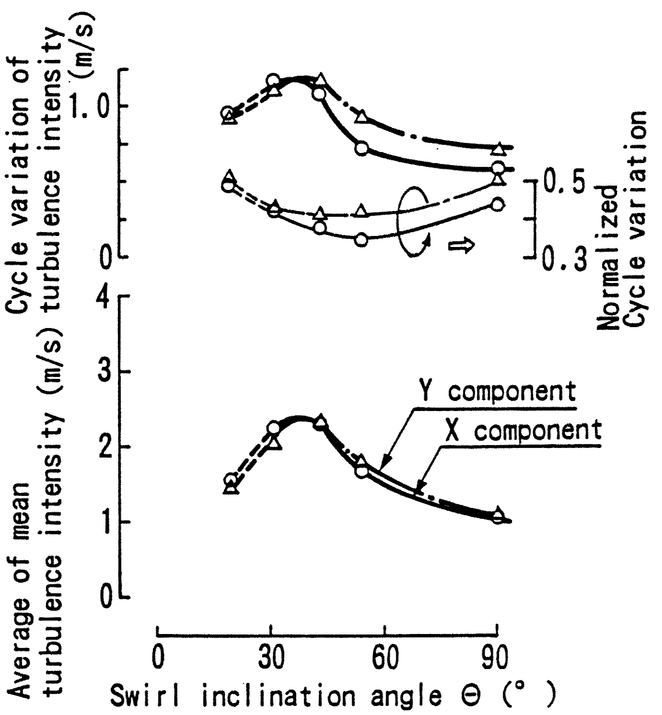

Fig. 7f Comparison of X & Y components

(Average of mean value for each degree of crank angle from TDC to 30°ATDC)

Fig.7 Effects of swirl inclination angle on mean turbulence intensity

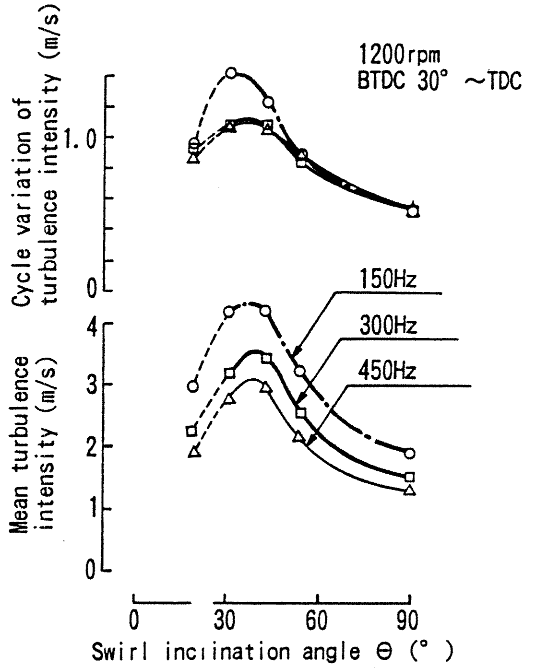

Fig.8 Influence of cut-off frequency (X component)

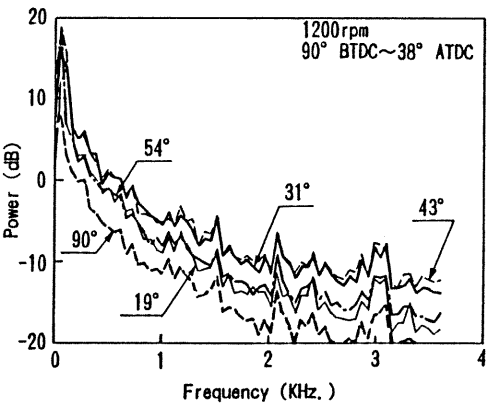

Fig.9 Mean power spectra characteristics (X component)

DISCUSSION

As stated above, from 30°BTDC to 30°ATDC the peak intensity value of both the X and Y components of turbulence occurs when the swirl is inclined between 30° and 45°. One of the possible explanations for this tendency is as follows: The turbulence generation mechanisms are different between the horizontal swirl and the vertical swirl at near TDC. It is thought that in the case of horizontal swirl, the shear stress between the gas flow and the combustion chamber walls generates turbulence, whereas in the case of vertical swirl, the turbulence is enhanced by the crushing of the swirling gas flow as the piston nears TDC. As explained in Fig.6, the vertical component of the angular momentum has a peak between θ =40° and 60°, and the horizontal component decreases as the swirl inclination angle θ increases. The efficiency of the conversion from angular momentum to turbulence, however, is higher for the vertical component than the horizontal component because of the difference in the turbulence generation mechanisms(10). Hence, the turbulence intensity as a combination of the turbulence converted from these vertical and horizontal components shows similar peak as vertical component between 30° and 45° which is slightly shifted from the peak of the vertical component of the angular momentum.

SUMMARY

The effects of the swirl inclination angle on the angular momentum and the turbulence characteristics of the flow in the 4-valve single cylinder engine with SCV and the pent roof combustion chamber was investigated using a backward-scatter LDV system with a very high data rate (max 20kHz). The findings were as follows:

1) Under a constant air flow rate, total angular momentum decreases as swirl inclination angle is increased. And the vertical component of the angular momentum has a peak between the swirl inclination angle of 40° and 60°, and the horizontal component decreases as the swirl inclination angle increases.
2) The peak value of turbulence intensity (measured in the center of the combustion chamber) corresponds to a swirl inclination angle between 30° and 45°.

REFERENCE

1. Okano, H., et al, "Toyota Lean-Burn System -Recent Development-," 11th Int. Vienna Motor Symposium, 1990.
2. Inoue, T., et al, "In Cylinder Gas Motion, Mixture Formation and Combustion of 4 Valve Lean Burn Engine," 9th Int. Vienna Motor Symposium, 1988.
3. Furuno, S., et al, "Swirl Motion Analysis in a Spherical Combustion Chamber, "IMechE, Combustion in Engines, C44, pp165-172, 1988-3.
4. Bracco, F. V., "Modeling and Diagnostics of Combustion in Spark-Ignition Engines, "COMODIA 85, pp1-14, 1985.
5. Fraser, R. A., et al, "Cycle-Resolved LDV Integral Length Scale Measurements Investigating Clearance Height Scaling, Isotropy, and Homogeneity in an I. C. Engine," SAE, Paper No.890615, 1989.
6. Glover, A. R., et al, "An Investigation into Turbulence in Engines using Scanning LDA," SAE, Paper No.880379, 1988.
7. Lorenz, M. et al, "Cycle Resolved LDV Measurements on a Fired SI-Engine at High Data Rates Using a Conventional Modular LDV-System, "SAE, Paper No.900054, 1990.
8. Ball, W. F., et al, "Laser Doppler Velocimeter Measurements of Turbulence in a Direct-injection Diesel Combustion Chamber," IMechE, Combustion in Engineering, Vol.I, C52, pp163-174, 1983-3.
9. Yamada, T., et al, "In-cylinder Gas Motion and Combustion in a 4 valve Lean Burn Engine," JSAE, 882, No.882092, pp367-370, 1988.
10. Arcoumanis, C., et al "Tumbling Motion: Avmechanism for Turbulence Enhancement in Spark-Ignition Engines," SAE Paper No.900060, 1990.
11. Khalighi, B., "Intake-Generated Swirl and Tumble Motions in a 4-valve Engine with Various Intake Configurations -Flow Visualization and Particle Tracking Velocimetry-," SAE, Paper No.900059, 1990.